Journal of Catalysis 320 (2014) 33–41

Contents lists available at ScienceDirect

Journal of Catalysis

journal homepage: www.elsevier.com/locate/jcat

Selective, one-pot catalytic conversion of levulinic acid to pentanoic acid over Ru/H-ZSM5

Wenhao Luo, Pieter C.A. Bruijnincx *, Bert M. Weckhuysen *

Inorganic Chemistry and Catalysis, Debye Institute for Nanomaterials Science, Utrecht University, Universiteitsweg 99, 3584 CG Utrecht, The Netherlands

ARTICLE INFO

Article history:
Received 17 June 2014
Revised 8 September 2014
Accepted 19 September 2014

Keywords:
Levulinic acid
Pentanoic acid
ZSM5
Ruthenium
Acidity
Catalyst synthesis

ABSTRACT

The direct conversion of levulinic acid (LA) to pentanoic acid (PA) has been studied with six 1 wt% Ru/H-ZSM5 catalysts at 40 bar H_2 and 473 K in dioxane. The influence of ZSM5 cation form, Si/Al ratio and ruthenium precursor on metal dispersion and acidity has been assessed. A highly active bifunctional 1 wt% Ru/H-ZSM5 catalyst was developed to give a PA yield of 91.3% after 10 h. The PA productivity of 1.157 $mol_{PA}\ g_{Ru}^{-1}\ h^{-1}$ is the highest reported to date. The simple preparation method allows for a significant fraction of ruthenium to be located inside the zeolite pores, providing the desired proximity between the hydrogenation function and the strong acid sites, which is key to the conversion of LA into PA. Coke buildup during reaction causes some deactivation, but activity can be almost fully restored after catalyst regeneration by simple coke burn-off.

1. Introduction

Levulinic acid (LA) has emerged as one of the most promising renewable platform molecules. Indeed, it provides many opportunities for biobased fuel and bulk chemicals production [1,2] and can be produced easily and economically from the carbohydrate fraction of lignocellulosic biomass through a simple and high yielding acid hydrolysis process [3]. Several derivatives of LA have been studied as cellulosic fuels or fuel additives; these include γ-valerolactone (GVL) [4], 2-methyltetrahydrofuran (MTHF) [5], pentanoic acid (PA) and its esters (PE) [6], all of which can be obtained by sequential LA hydrodeoxygenation steps (Scheme 1). While GVL has received most attention, two recent examples have demonstrated that pentenoic/pentanoic acid-based value chains are also very promising for the production of cellulosic biofuels [7].

Lange et al. showed, for instance, that so-called valeric biofuels, i.e., pentanoic acid esters, are a superior class of cellulosic biofuels [6]. A multistep catalytic conversion of LA into valeric esters was reported, involving the hydrogenation of LA to GVL over Pt/TiO_2, the conversion of GVL to PA by acid-catalyzed ring-opening and the hydrogenation over a bifunctional Pt/H-ZSM5 catalyst and, finally, esterification to the desired pentanoic acid esters (PE) over an acidic ion exchange resin. In addition to PE synthesis, a comprehensive study of their fuel properties was conducted, which demonstrated the compatibility of PE for both gasoline and diesel applications and revealed a superior performance [6].

The Dumesic group also reported on the production of PA, in this case from GVL over a bifunctional Pd/Nb_2O_5 catalyst [8]. PA could subsequently be converted into 5-nonanone, i.e., by ketonization and ultimately to hydrocarbon fuels suitable for gasoline and diesel applications [8]. Both approaches thus consist of a two-step conversion of LA into PA and require a catalyst system combining an acid functionality and a hydrogenation function for the second, most difficult step, i.e., the ring-opening/hydrogenation of GVL to PA.

Building on these results, we previously reported on the direct, one-pot conversion of LA to PA and PE, without isolating the GVL intermediate, using bifunctional catalysts consisting of ruthenium supported on H-ZSM5 or H-β. A yield of 45.8 mol% of PA was obtained with 1 wt% Ru/H-ZSM5 in dioxane at 473 K and after 4 h of reaction time [9]. An extensive catalyst deactivation study showed that acid site loss as the result of dealumination is the cause of deactivation under the applied conditions, which involved elevated temperatures and a highly polar and corrosive environment. Relatedly, Pan et al. recently reported the direct conversion of LA to valeric acid and its ester, performing the reaction in ethanol over various bifunctional ruthenium catalysts with 5 wt% Ru/SBA-SO_3H performing best with a combined PA/PE yield of 94%

* Corresponding authors. Fax: +31 (0)30 251 1027.
E-mail addresses: p.c.a.bruijnincx@uu.nl (P.C.A. Bruijnincx), b.m.weckhuysen@uu.nl (B.M. Weckhuysen).

http://dx.doi.org/10.1016/j.jcat.2014.09.014
0021-9517/

at 523 K after 6 h of reaction, after a comprehensive optimization of the reaction conditions [10]. Also for this catalyst system, acid site loss was found to be an issue. These first, few examples nonetheless show that the direct conversion is feasible and the promising results warrant further exploration.

The efficient conversion of LA to PA requires a careful balance to be struck between the number, strength, and location of the acid and hydrogenation sites, key parameters that in principle can be controlled by careful catalyst synthesis. Herein, we further explore 1 wt% Ru/H-ZSM5 as a catalyst for the direct conversion of LA to PA and study the influence of catalyst preparation on activity and selectivity. H-ZSM5 was selected as the acidic support, given its higher intrinsic acid strength than H–Y [11] and the fact that acid leaching (dealumination) was previously found to be more limited with H-ZSM5 than with H-β under the demanding conditions required for the LA to PA conversion [9]. In the sequential hydrodeoxygenation of LA to PA (Scheme 1), LA can be first converted to GVL, either via ring closure and subsequent hydrogenation involving angelicalactone (AL) as intermediate or via hydrogenation first to 4-hydroxypentanoic acid (HPA) followed by ring closure; GVL can subsequently be ring-opened to PEA and finally hydrogenated to PA; an alternative route differs in the fate of the first intermediate 4-hydroxypentanoic acid (HPA), which can in principle also be directly dehydrated to PEA, followed finally by hydrogenation to PA [12,13]. The strong acidity of the zeolite would be important for both routes. Putting the strong acid sites and hydrogenation metal in close proximity might furthermore favor the second LA–HPA–PEA–PA route and thus avoid the most difficult step of both sequences, i.e., GVL ring-opening. To achieve this, controlled deposition/exchange of ruthenium, especially into the zeolite pores is required.

Here, we report on the influence of preparation method and zeolite composition on the catalytic performance and stability of 1 wt% Ru/H-ZSM5 catalysts for the LA to PA conversion. The influence of the type of extra-framework cations in ZSM5 before wet impregnation, ruthenium precursor, and variation of Si/Al ratio was examined on (1) metal dispersion and distribution, (2) H-ZSM5 acidity, and (3) catalytic performance of the Ru/H-ZSM5 catalysts in the direct, one-pot conversion of LA to PA in dioxane at 473 K. A much improved bifunctional catalyst was developed by a new, simple synthesis method to yield 91.3% PA within a reaction time of 10 h. A comparison of catalysts of varying acidity showed acid strength to be key to the efficient conversion of LA to PA. Finally, insight into the activity, stability, and deactivation of the new 1 wt% Ru/H-ZSM5 catalysts is provided.

2. Experimental section

2.1. Catalyst preparation

Six distinct 1 wt% Ru/H-ZSM5 catalysts were prepared via a wet impregnation method. The required amount of precursor solution (22 mL) was prepared with deionized water in a 50-mL round bottom flask equipped with a magnetic stirring bar. The round bottom flask was submerged in a temperature controlled oil bath, and the mixture was then agitated at 303 K using a hot plate stirrer (1000 rpm). After 10 min of stirring, the ZSM5 support was slowly added to the impregnation solution, with agitation speed 1000 rpm at 303 K for about 1 h. After mixing of the support with the impregnation solution, the temperature was raised to 358 K and kept at that temperature for 12 h, allowing evaporation of the solvent at a desirable rate. A fine catalyst powder was obtained of homogeneous color, which was then reduced directly at 723 K with a heating ramp 2 K/min under a flow of 10 vol.% H_2/N_2 for 6 h. The catalyst sample was subsequently cooled rapidly to room temperature and used without any further modification.

The six 1 wt% Ru/H-ZSM5 catalysts are labeled according to their preparation method. The first indicator denotes the ruthenium precursor used with 'Cl'/'NH_3' indicating $RuCl_3$ (99.9%, Acros Chemicals)/$Ru(NH_3)_6Cl_3$ (99%, ABCR), respectively; the second indicator, 'A'/'H', indicates if the cation of the ZSM5 support was either NH_4^+ or H^+ prior to impregnation; the last indicator depicts the Si/Al ratio of ZSM5. Four ZSM5 materials were used in this study with Si/Al ratios of 11.5 (CBV2314, S_{BET} = 425 m^2/g), 25 (CBV5524G, S_{BET} = 425 m^2/g), 40 (CBV8014, S_{BET} = 425 m^2/g), 140 (CBV28014, S_{BET} = 400 m^2/g; all from Zeolyst).

Two 1 wt% Ru/H-ZSM5 catalysts, Ru/H-ZSM5(Cl, H, 11.5) and Ru/H-ZSM5(Cl, A, 11.5) were prepared with $RuCl_3$ as the ruthenium precursor and CBV2314 as the support; for Ru/H-ZSM5(Cl, H, 11.5), the ammonium form of ZSM5 was converted to H-ZSM5 before impregnation by heating NH_4-ZSM5 at 1 K/min to 393 K for 1 h and at 2 K/min to 823 K for 4 h; the other four 1 wt% Ru/H-ZSM5 catalysts were prepared with $Ru(NH_3)_6Cl_3$ as precursor and used the ammonium form of the four ZSM5 zeolites of different Si/Al ratio: Ru/H-ZSM5(NH_3, A, 11.5), Ru/H-ZSM5(NH_3, A, 25), Ru/H-ZSM5(NH_3, A, 40), and Ru/H-ZSM5(NH_3, A, 140).

For comparison, a parent ZSM5 (11.5) sample (CBV2314), without having been impregnated, was similarly treated at 723 K with a heating ramp of 2 K/min under a flow of 10 vol.% H_2/N_2 for 6 h. Catalyst regeneration of spent Ru/H-ZSM5(NH_3, A, 11.5) was performed by heating the spent catalyst to 723 K with a heating ramp of 2 K/min under a flow of 10 vol.% H_2/N_2 for 4 h.

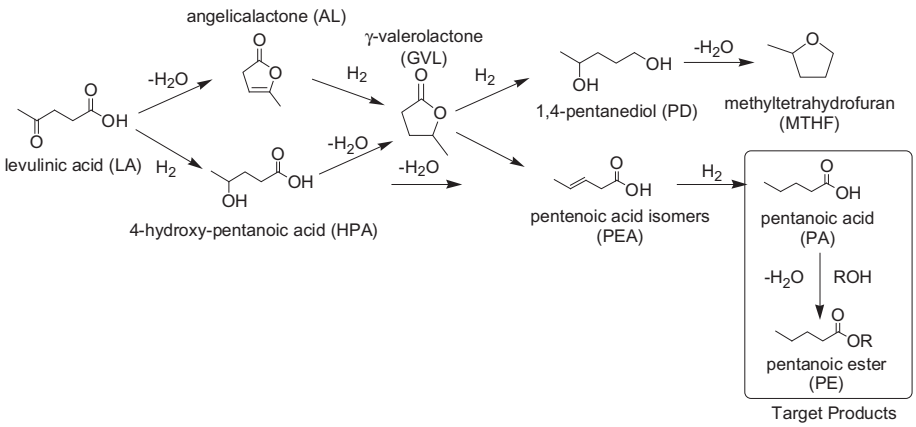

Scheme 1. Levulinic acid hydrodeoxygenation platform.

2.2. Catalyst characterization

2.2.1. Transmission electron microscopy (TEM)

The bright field and high angle annular dark field (HAADF) TEM images were obtained using a Tecnai 20FEG microscope operating at 200 kV. Ruthenium particle diameters of more than 200 particles for each sample were measured using the iTEM software (soft Imaging System GmbH). For non-symmetrical particle shapes, both the largest and shortest diameter were measured to obtain an average value.

2.2.2. N_2 physisorption

N_2 physisorption isotherms were recorded to determine surface areas and pore volumes using a Micromeritics Tristar 3000 set-up operating at 77 K. All samples were outgassed for 12 h at 473 K in a nitrogen flow prior to the physisorption measurements. BET surface areas were determined using 10 points between 0.06 and 0.25. Micropore volumes (cm^3/g) were determined by *t*-plot analysis for *t* between 3.5 and 5.0 Å to ensure inclusion of the minimum required pressure points.

2.2.3. Temperature-programmed desorption of ammonia (TPD-NH_3)

Catalyst acidity was investigated by TPD-NH_3 under He flow (25 mL/min) using a Micromeritics AutoChem II equipped with a TCD detector. 0.15–0.2 g of catalyst was loaded and dried at 873 K for 1 h, after which the sample was cooled down to 373 K. Subsequently, pulses of ammonia were introduced up to saturation of the sample. The temperature-programmed desorption was performed up to 873 K, with a heating ramp of 5 K/min. The total number of acid sites (mmol NH_3/gram zeolite) was determined from the total amount of desorbed ammonia.

2.2.4. Thermal gravimetric analysis (TGA)

TGA-MS measurements of the spent catalysts were performed with a Perkin–Elmer Pyris 1 apparatus. The sample was initially heated to 423 K for 1 h with a temperature ramp of 10 K/min in a 20 mL/min flow of argon to exclude physisorbed water and acetone, followed by a ramp of 5 K/min to 973 K in a 10 mL/min flow of oxygen to burn off the coke. Analysis was performed with a quadrupole Pfeiffer Omnistar mass spectrometer, which was connected to the outlet of the TGA apparatus. Ion currents were recorded for *m*/*z* values of 18 and 44.

2.3. Catalyst activity and stability testing

LA hydrodeoxygenation reactions were conducted in a 100 mL Parr batch autoclave reactor equipped with a thermocouple, a pressure transducer and gauge and overhead stirring. In a typical run, the batch reactor was loaded with a 10 wt% levulinic acid solution (6.0 g, 51.7 mmol) in dioxane (54 g) and the 1 wt% Ru catalyst (0.6 g). The reactor was sealed, purged three times with argon, heated to 473 K and subsequently charged with H_2 to 40 bar. This was taken as the starting point of the reaction. Reactions were run for 10 h with a stirring speed of 1600 rpm; this stirring speed was previously shown to be sufficient for avoiding external mass transfer limitations, guarantying the reactions to be operated in the kinetic regime [9]. After the reaction, the autoclave was cooled to room temperature, H_2 was released and 2 wt% anisole was added as internal standard. The catalyst was separated by centrifugation, filtration, and finally washed with acetone.

The experiments that aimed at higher PA yields as well as the stability tests were run at a higher catalyst loading. These reactions were conducted in a 50 mL Parr batch autoclave reactor at 473 K for 10 h using a hydrogen pressure of 40 bar and a stirring speed of 1600 rpm. These runs were performed with 10 wt% levulinic acid (2.5 g, 21.5 mmol) in dioxane (22.5 g) over 1 wt% Ru/ZSM5 11.5 catalysts (0.5 g).

The reaction products were analyzed using a Varian gas chromatograph equipped with a VF-5 ms capillary column and FID detector. Products were identified with a Shimadzu GC–MS with a VF-5 ms capillary column. The gas phase reaction products were analyzed by an online dual channel Varian CP4900 micro-GC equipped with a CO_X column and TCD detector, for analysis of H_2, CO_2, CO, and CH_4.

3. Results and discussion

A series of six distinct 1 wt% Ru/H-ZSM5 catalysts were prepared, by varying the cation form and Si/Al ratio of the zeolite as well as the ruthenium precursor salt, and tested in the hydrodeoxygenation of LA. The influence of the extra-framework cation (NH_4^+ vs. H^+) of the ZSM5 support with a Si/Al ratio of 11.5 and impregnation salt ($RuCl_3$ vs. $Ru(NH_3)_6Cl_3$) on the catalysts' physicochemical properties and performance were assessed by comparison of Ru/H-ZSM5(Cl, H, 11.5), Ru/H-ZSM5(Cl, A, 11.5), and Ru/H-ZSM5(NH_3, A, 11.5). Four different Si/Al ratios varying from 11.5 to 40 were examined with Ru/H-ZSM5(NH_3, A, 11.5), Ru/H-ZSM5(NH_3, A, 25), Ru/H-ZSM5(NH_3, A, 40), and Ru/H-ZSM5(NH_3, A, 140), all prepared with the $Ru(NH_3)_6Cl_3$ precursor and the zeolites in the ammonium form. As ruthenium is known to form the volatile oxides RuO_2 and RuO_4, and to severely sinter when contacted with oxygen above 373 K [14], the traditional calcination step was omitted and the wet impregnation step was followed directly by a prolonged reduction step of 6 h, in order to fully decompose the ruthenium precursor and prepare catalysts with a better dispersion of ruthenium.

3.1. Physicochemical characterization of the catalysts

The physicochemical properties of the six catalysts under study are given in Table 1. Ruthenium particle sizes, falling in the range of 1.7–4.9 nm, and dispersions were determined by TEM (Fig. S1). The number and strength of acid sites of the parent zeolite ZSM5 (11.5) and the six zeolite-supported catalysts were determined by temperature-programmed desorption of ammonia (TPD-NH_3, Fig. 1, Table 2). The TPD-NH_3 traces could be divided into two clearly distinguishable parts, with desorption being observed at a low-temperature range (LT) from 430 to 580 K and a high-temperature range (HT) from 590 to 740 K. These LT and HT ranges correspond to weak and strong acid sites, respectively [15,16].

The metal dispersion as well as the acidity of the catalyst was found to depend strongly on the cation in the zeolite used for the impregnation step. Ru/H-ZSM5(Cl, H, 11.5), for instance, showed a ruthenium dispersion of 0.39 (average particle size of 3.3 nm), which was slightly better than that of Ru/H-ZSM5(Cl, A, 11.5) 0.26 (particle size of 4.9 nm). In both cases, ruthenium particles can be mainly found at the external surface of the zeolite. While giving a better Ru dispersion, a significant decrease in strong acid sites (HT) with concomitant large increase in weak acid sites (LT) was seen when H^+-type ZSM5 was used for the impregnation (Fig. 1). This is undesirable as strong acid sites are essential to efficient PA production. Ru/H-ZSM5(Cl, H, 11.5) actually contained the largest amount of LT (0.23 mmol/g_{cat}) and lowest amount of HT (0.34 mmol/g_{cat}) of the three catalysts made with the Si/Al = 11.5 ZSM5 support (Table 2, entry 2–4). If one takes into account that a sample of bare NH_4^+-ZSM5 zeolite subjected to the same reduction conditions as the other ruthenium-loaded zeolites contains 0.57 HT and 0.04 mmol/g_{cat} LT (Table 2, entry 1), then it is clear from the results above that conversion of the zeolite from NH_4^+ to H^+ form prior to impregnation is not beneficial, given the resulting

Table 1
Physicochemical properties of fresh Ru/H-ZSM5 and spent catalysts after reaction at 473 K, 40 bar H_2 after 10 h in dioxane.

	Catalyst	BET (m^2/g)		Micropore surface area (m^2/g)		Micropore volume (cm^3/g)[a]		Pore volume (cm^3/g)[b]		Average Ru particle size (nm)[c]		Ru dispersion ZSM5[d]		Coke contents (wt%)[e]
1	Non-impregnated ZSM5 (11.5)	379		295		0.14		0.22		–		–		–
	Ru/H-ZSM5	Fresh	Spent	Fresh	Spent	Fresh	Spent	Fresh	Spent	Fresh	Spent	Fresh	Spent	
2	(Cl, H, 11.5)	333	126	247	112	0.12	0.06	0.20	0.09	3.3 ± 1.4	6.6 ± 2.6	0.39	0.20	8.0
3	(Cl, A, 11.5)	371	53	266	51	0.13	0.03	0.23	0.05	4.9 ± 1.4	6.7 ± 2.2	0.26	0.19	9.2
4	(NH_3, A, 11.5)	324	137	251	107	0.12	0.05	0.19	0.06	1.7 ± 0.4	3.8 ± 0.9	0.76	0.34	7.6
5	(NH_3, A, 25)	377	208	242	137	0.12	0.07	0.26	0.18	4.3 ± 1.5	5.0 ± 1.9	0.30	0.26	5.8
6	(NH_3, A, 40)	390	267	237	161	0.12	0.08	0.27	0.21	4.8 ± 1.6	6.1 ± 2.0	0.27	0.21	4.0
7	(NH_3, A, 140)	363	337	221	168	0.11	0.08	0.21	0.20	6.2 ± 3.2	7.4 ± 1.9	0.21	0.17	1.6

[a] Data obtained by the t-plot method.
[b] Data obtained by single point adsorption.
[c] Data obtained by TEM.
[d] Data estimated by TEM: $D = 6 * (v_m/a_m)/d$. Where v_m is bulk metal atomic density of Ru (13.65×10^{-3} nm^3), a_m is the surface area occupied by an atom on a polycrystalline surface of Ru (6.35×10^{-2} nm^2), d is the cluster size of Ru metal.
[e] Data determined by TGA.

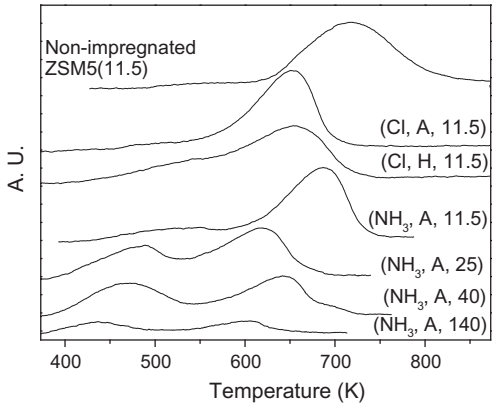

Fig. 1. TPD-NH_3 profiles of the parent ZSM5 and the six 1 wt% ZSM5-supported catalysts.

large drop in acid strength. This transition of strong acid sites to weak ones during the pretreatment process at 823 K was attributed to the extraction of framework aluminum species (Fig. 1) [17]. The use of NH_4^+-ZSM5 is therefore preferred for the synthesis of the bifunctional catalyst.

The Ru dispersion could be further improved by using $Ru(NH_3)_6Cl_3$ as precursor on NH_4^+-ZSM5 to give Ru/H-ZSM5(NH_3, A, 11.5). This preparation method gave the smallest average particle size of 1.7 nm of all the Ru/H-ZSM5 catalysts, with concomitant significant increase in Ru dispersion to 0.76 (Table 1, entry 4). Previous studies also showed that large ruthenium particles were obtained by impregnation of X, L, and ZSM5 zeolites with ruthenium chloride after calcination and H_2-reduction [18], while small ruthenium clusters could be obtained by ion exchange of Na^+-Y zeolites with aqueous solutions of $Ru(NH_3)_6Cl_3$ [14,19–21]. The higher dispersion obtained with $Ru(NH_3)_6Cl_3$ was thought to be the result of strong interaction between negatively charged porous framework of ZSM5 and the ruthenium cations formed upon dissolution of $Ru(NH_3)_6Cl_3$ in water; conversely, the lower dispersions and larger particle sizes observed outside of ZSM5 with $RuCl_3$ are the result of weaker interactions between metal salt and support [18]. An additional, important benefit of using $Ru(NH_3)_6Cl_3$ is that with this precursor, the largest amount of strong acid sites is preserved (0.48 mmol/g). Indeed, the temperature of maximum ammonia desorption in the HT region is at 686 K, which is the closest to the maximum of 719 K observed for the original, non-impregnated zeolite (Table 2, entry 4). The use of $Ru(NH_3)_6Cl_3$ thus improved metal dispersion as well as efficiently preserved the amount and strength of strong acid sites on ZSM5.

Variation of the zeolite's Si/Al ratio was also found to affect ruthenium dispersion. Expectedly, the total number of acid sites and fraction of strong acid sites of the 1 wt% Ru/H-ZSM5 catalysts decreased with increasing the Si/Al ratio from 11.5 to 140 (Table 2, entry 4–7). The average ruthenium particle size in turn was found to gradually increase from 1.7 to 6.2 nm with increasing Si/Al ratio (Table 1, entry 4–7). A similar increase in average particle size from 1.4 to 6.1 nm upon increasing the Si/Al ratio from 11.5 to 500 was also seen by You et al. [22] for platinum supported on ZSM5. The difference in the distribution of strong and weak acid sites might be responsible for the observed differences in the Ru dispersion, with those zeolites richer in HT sites stabilizing smaller Ru clusters. For Pt/H-ZSM5 it is known, for instance, that highly acidic zeolites lead to higher Pt dispersion, with computational studies pointing at the stabilizing interaction between Pt and a Brønsted acidic proton [23].

Table 2
Amount and type of acid sites as determined by NH_3-TPD.

	Catalyst	LT region T of maximum desorption (K)	Amount of weak acid sites (mmol/g_{cat})	HT region T of maximum desorption (K)	Amount of strong acid sites (mmol/g_{cat})	Total acidity (mmol/g_{cat})
1	Non-impregnated ZSM5 (11.5)	559	0.04	719	0.57	0.61
	Fresh Ru/H-ZSM5					
2	(Cl, H, 11.5)	544	0.23	657	0.34	0.57
3	(Cl, A, 11.5)	575	0.10	655	0.44	0.54
4	(NH_3, A, 11.5)	517	0.12	686	0.48	0.60
5	(NH_3, A, 25)	476	0.20	615	0.31	0.51
6	(NH_3, A, 40)	467	0.25	636	0.24	0.49
7	(NH_3, A, 140)	434	0.07	597	0.07	0.14

Additional insights into the distribution of ruthenium might be obtained from any observed decrease in pore volume and the number of acid sites, as these changes give an indication of the fraction of small ruthenium clusters deposited/exchanged into the ZSM5 pores, i.e., those that are difficult to be visualized in TEM. Zhao et al., for instance, previously reported on a decrease in pore volume and acid density of ZSM5 when a significant fraction of Ni was located inside the ZSM5 pores [24]. A similar decrease, reported by You et al. after introduction of platinum [22] on ZSM5, was again attributed to the fraction of Pt deposited inside the ZSM5 pores. The surface areas and pore volumes of the Ru catalysts as determined by N_2 physisorption are listed in Table 1. Compared to the non-impregnated zeolite ZSM5(11.5), wet impregnation of ZSM5(11.5) with Ru with the different precursors resulted in a drop in pore volume and acid density in most cases (Tables 1 and 2), indicating the formation of small Ru particles inside the zeolite pores. The pore volume of ZSM5(11.5) dropped from 0.22 to 0.20 cm^3/g and 0.19 cm^3/g for Ru/H-ZSM5(Cl, H, 11.5) and Ru/H-ZSM5(NH_3, A, 11.5), respectively (Table 1, entry 1, 2, 4), whereas no loss in pore volume was observed for Ru/H-ZSM5(Cl, A, 11.5). The 0.02 cm^3/g decrease in pore volume observed for Ru/H-ZSM5(Cl, H, 11.5) might also have an additional origin. A significant increase in the fraction of weak acid sites is seen for this catalyst, which points at a partial pore blockage by migration of Al to extra-framework sites upon transition of the NH_4^+-ZSM5 to the H^+-ZSM5 prior to impregnation [17,25]. The drop in pore volume and much better ruthenium dispersion for Ru/H-ZSM5(NH_3, A, 11.5) indicate that this catalyst has the largest fraction of Ru particles deposited inside the zeolite channel system.

3.2. Catalytic performance

Catalytic activity of the six 1 wt% Ru/H-ZSM5 catalysts was initially compared at 473 K and 40 bar H_2 with a 10 wt% solution of LA in dioxane and a stirrer speed of 1600 rpm, conditions that are identical to those of our previous study. As reported, dioxane decomposition takes place to a limited extent in the presence of strongly acidic catalysts, yielding ethanol, 2-ethoxyethanol, and butanol as decomposition products, among others. The secondary PE products that are formed with these solvent-derived alcohols (up to 25 mol% max.) should be considered as PA and are included in the total PA yields reported below. The activity of the catalysts is reported in Table 3 in terms of PA productivity, expressed as $mol_{PA}\ g_{Ru}^{-1}\ h^{-1}$. The time online concentration profiles of substrate and products are depicted in Fig. 3. Trace amounts of MTHF were found, but no PD was observed in any of the reactions, indicating that the LA–GVL–MTHF route is insignificant over the 1 wt% Ru/H-ZSM5 catalysts under the applied conditions. As can be seen from the time profiles, GVL is initially formed as the primary product, with selectivity to PA increasing over time as a result of the consecutive hydrodeoxygenation reaction.

The variations in metal location, dispersion, and acidity as a result of the different preparation methods are clearly reflected in the catalytic activity and PA productivity (Fig 2a–c). For example, Ru/H-ZSM5(Cl, A, 11.5) gave a higher PA yield of 23.3 mol% PA and productivity of 0.451 $mol_{PA}\ g_{Ru}^{-1}\ h^{-1}$ than Ru/H-ZSM5(Cl, H, 11.5) did (7.2 mol% and 0.250 $mol_{PA}\ g_{Ru}^{-1}\ h^{-1}$) after 10 h of reaction (Fig. 2a, b and Table 3, entry 1, 2). It should be noted that Ru/H-ZSM5(Cl, A, 11.5) has more strong acid sites but a lower metal dispersion than Ru/H-ZSM5(Cl, H, 11.5). This implies that acidity plays a more important role than ruthenium dispersion in PA production, which is in an agreement with our previous study in which the acid-catalyzed GVL ring-opening was shown to be rate-limiting [9]. Ru/H-ZSM5(NH_3, A, 11.5) gave a PA yield of 57.4 mol%, showing that the change of ruthenium precursor in the preparation method resulted in a rather substantial increase in PA production. More importantly, the rate of PA formation does not seem to slow down, even after 10 h of reaction time; this in contrast to Ru/H-ZSM5(Cl, H, 11.5) which already shows some signs of deactivation after 3 h of reaction (Fig. 2a and c). The use of $Ru(NH_3)_6Cl_3$ as the precursor thus clearly improves catalyst performance in terms of PA yield. Based on the characterization data discussed above, this can be attributed to the good preservation of strong acid sites and the improved deposition of ruthenium particles also inside the zeolite pores leading to close proximity of the active sites in the bifunctional catalyst.

Table 3
One-pot hydrodeoxygenation of levulinic acid (LA) to pentanoic acid (PA).

	Catalyst	C-balance (%)	LA conv. (%)	GVL yield (%)	PA yield (%)[a]	Productivity ($mol_{PA}\ g_{Ru}^{-1}\ h^{-1}$)
Catalyst screening[b]						
1	(Cl, A, 11.5)	93.3	100	70.0	23.3 (4.7)	0.451
2	(Cl, H, 11.5)	98.8	100	91.6	7.2 (0.9)	0.169
3	(NH_3, A, 11.5)[d]	88.7	100	31.3	57.4 (17.7)	0.629
4	(NH_3, A, 25)	76.4	97.9	50.1	24.2 (8.0)	0.135
5	(NH_3, A, 40)	86.8	97.5	68.0	16.3 (4.5)	0.131
6	(NH_3, A, 140)	88.0	72.2	58.2	1.0 (0.0)	0.009
PA yield optimization for (NH_3, A, 11.5) and catalyst reuse[c]						
7	1st run[d]	99.0	100	7.7	91.3 (25.0)	1.042
8	2nd run	94.3	100	21.3	66.4 (17.7)	0.547
9	3rd run after coke burn-off	91.1	100	9.9	81.2 (25.2)	0.685
Comparison with literature results						
10[e]	(NH_3, A, 11.5)	93.4	100	28.9	64.5 (18.9)	1.157
11[e]	1 wt% Ru/H-ZSM5	96.0	100	50.2	45.8 (16.3)	0.822
12[f]	5 wt% Ru/SBA-SO_3H	100	100	4.0	90.0	0.060[g] 0.160[h]
13[g]	5 wt% Ru/H-ZSM5	93.0	99.0	43.0	49.0	0.033

[a] The total PA yield is given; this value includes the PE yield which is given in parentheses.
[b] Conditions: 1 wt% Ru/H-ZSM5, 51.7 mmol of LA, 0.6 g of catalyst, 54 g dioxane, 10 h, 473 K and 40 bar H_2.
[c] Conditions: 1 wt% Ru/H-ZSM5, 21.5 mmol of LA, 0.5 g of catalyst, 22.5 g dioxane, 10 h, 473 K and 40 bar H_2.
[d] See Fig. S2 for dependence of productivity on catalyst/substrate ratio.
[e] Conditions: 21.5 mmol of LA, 0.3 g of catalyst, 22.5 g dioxane, 4 h, 473 K and 40 bar H_2. See Ref. [9] for details.
[f] Conditions: 4 mmol of LA, 0.2 g of catalyst, 10 mL of ethanol, 6 h, 523 K and 40 bar H_2. See Ref. [10] for details.
[g] PA productivity obtained after 6 h reaction time at 523 K.
[h] Highest PA productivity obtained at 513 K. See Ref. [10] for details.

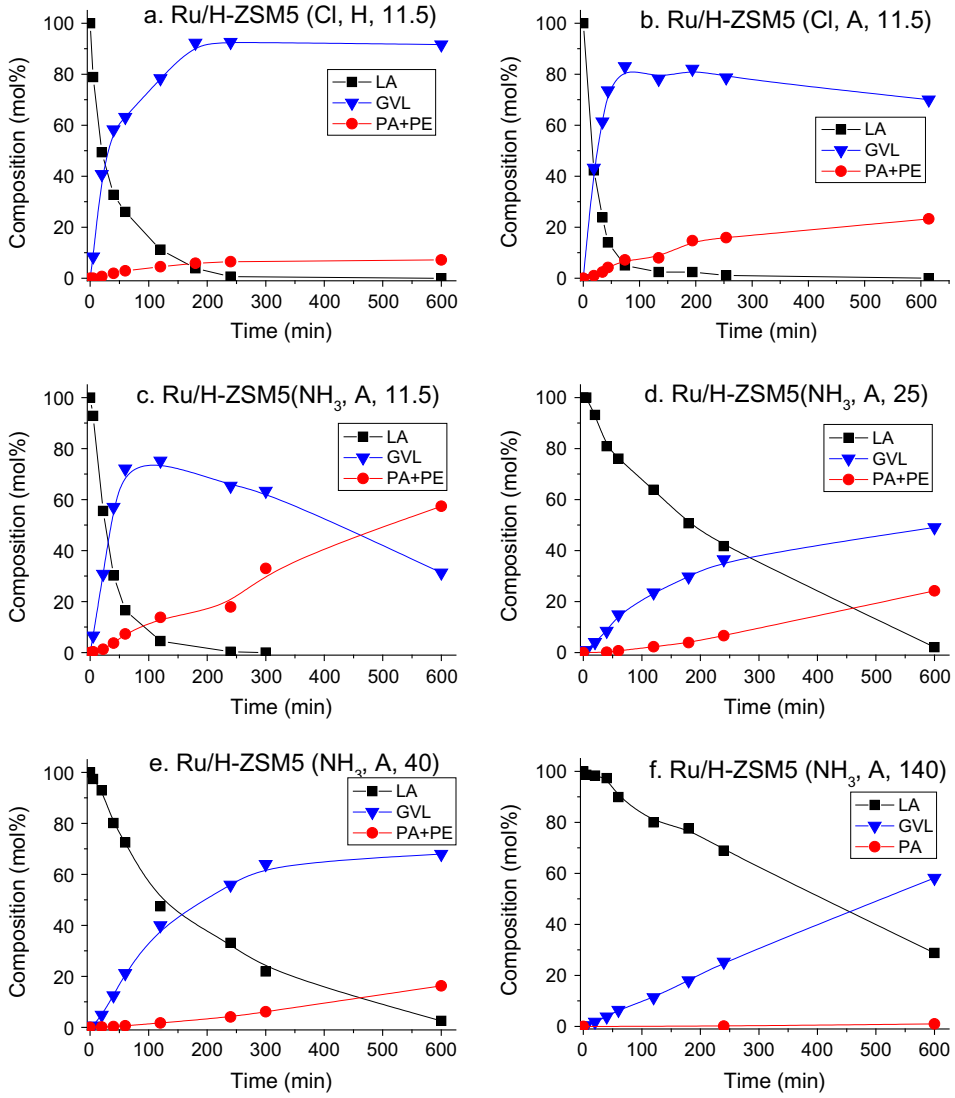

Fig. 2. Time profiles of the catalytic hydrodeoxygenation of 10 wt% LA in dioxane at 473 K and 40 bar H_2 pressure, 1 wt% Ru/H-ZSM5, stirrer speed of 1600 rpm. LA: levulinic acid; GVL: γ-valerolactone; PA + PE: pentanoic acid and its esters.

Clear differences in selectivity and activity are also observed upon variation of the Si/Al ratio of ZSM5 (Fig. 2d–f and Table 3 entry 3–6). Full LA conversion was achieved with Ru/H-ZSM5 (NH_3, A, 11.5) after 5 h (Fig. 2c), while 2.1, 2.5, and 27.8 mol% of LA were still left after 10 h reaction with the catalysts with Si/Al ratios of 25, 40, and 140, respectively. PA productivity of the Ru/H-ZSM5 catalysts decreased accordingly, with Ru/H-ZSM5(NH_3, A, 140) having produced hardly any PA after 10 h. These results are in line with Pan et al. who also included a 5 wt% Ru/H-ZSM5 catalyst with a high Si/Al ratio of 50 in their screening studies and observed a low PA productivity of 0.033 $mol_{PA}\ g_{Ru}^{-1}\ h^{-1}$ at the higher reaction temperature of 513 K (Table 3, entry 13) [10].

The PA yield can be further improved with a slight increase in catalyst loading under otherwise standard conditions of 473 K and 40 bar H_2 (Fig. S2). A PA yield of 91.3 mol% could thus be achieved with 1 wt% Ru/ZSM5(NH_3, A, 11.5) after a 10 h reaction with an excellent mass balance of 99.0% (Table 3, entry 7), corresponding to a productivity of 1.042 $mol_{PA}\ g_{Ru}^{-1}\ h^{-1}$. This productivity is at least six fold higher than the highest PA productivity of 0.16 $mol_{PA}\ g_{Ru}^{-1}\ h^{-1}$ recently reported by Pan et al. for the production of PA + PE from LA over 5 wt% Ru/SBA-SO_3H, a reaction which was run at the higher temperature of 513 K (Table 3, entry 12) [10]. A 4 h run with 1 wt% Ru/H-ZSM5(NH_3, A, 11.5) allowed for a direct comparison with our previously reported Ru/H-ZSM5 catalyst (Table 3, entry 10 and 11), which was prepared with $RuNO(NO_3)_3$ as precursor via a wet impregnation method followed by both calcination and reduction [9]. The new results show that an improved yield and productivity can be obtained with the new catalyst (64.5 mol% PA/1.157 $mol_{PA}\ g_{Ru}^{-1}\ h^{-1}$ vs. 45.8 mol% PA/0.822 $mol_{PA}\ g_{Ru}^{-1}\ h^{-1}$).

The excellent activity of the 1 wt% Ru/H-ZSM5(NH_3, A, 11.5) catalyst in the direct, one-pot conversion of LA to PA can be mainly attributed to the improved dispersion of small ruthenium particles and the number and accessibility of the strong acid sites that are required for this reaction. The time online profiles with Ru/H-ZSM5(NH_3, A, 11.5) show (Figs. 2c and 3a) that only GVL is detected as intermediate in the reaction, which indicates

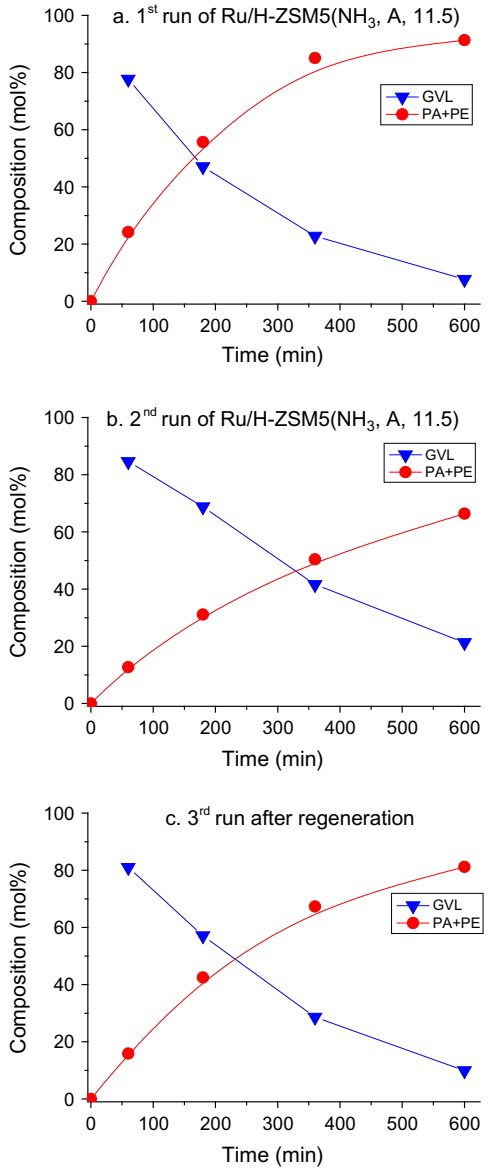

Fig. 3. Time profiles of the catalytic hydrodeoxygenation of 10 wt% LA in dioxane at 473 K, 40 bar H_2, 10 h reaction time, with wt% Ru/H-ZSM5(NH_3, A, 11.5), stirrer speed of 1600 rpm. GVL: γ-valerolactone; PA: pentanoic acid and its esters; LA conversion was 100% for all three runs within 1 h and is therefore not depicted.

that PA is dominantly formed via the LA–GVL–PEA–PA route. PA is, however, already detected at low LA conversions, which might indicate that the LA–HPA–PEA–PA route, which avoids the most difficult GVL–PEA step, also occurs, possibly facilitated by the close proximity of the ruthenium and strong acid sites in the H-ZSM5 pores. Although HPA is hard to detect due to its instability under the applied conditions, it has been reported that reactive intermediates can be stabilized in zeolites pores via confinement and nest effects [26–29]. The HPA intermediate might be stabilized by a strong acid site in the ZSM5 pores and subsequently directly dehydrated to PEA, rather than it being ring-closed to GVL. Dumesic et al. previously proposed the HPA to PEA route to be thermodynamically relevant at 523 K [13]. Recently, Xin et al. achieved a 95% selectivity of PA by the electrochemical reduction of LA to PA at pH = 0 on a Pb electrode in an electrocatalytic (flow) cell reactor, also suggesting the same LA–HPA–PEA–PA pathway [12].

3.3. Catalyst stability and reuse

The spent catalysts were characterized to detect any changes in either metal phase or zeolite support. The average ruthenium particle sizes are given in Table 1, with TEM pictures of the spent catalysts being depicted in Fig. S1. For all catalysts, different extents of sintering occurred as evidenced by the slight increase in ruthenium particle size after 10 h of reaction. We already previously observed that leaching of ruthenium is very limited under the employed reaction conditions [9].

The N_2 physisorption data (Table 1) show a significant drop in surface area of 62% and 86% for the spent Ru/H-ZSM5(Cl, H, 11.5) and (Cl, A, 11.5) catalysts, as a result of 8.0 wt% and 9.2 wt% coke build-up on the catalyst surface during reaction, as determined by TGA(-MS). Ru/H-ZSM5(NH_3, A, 11.5), the catalyst giving the best PA yield, suffered a little less from coke formation (7.6 wt%). Upon increase of the Si/Al ratio, the amount of coke deposited was found to decrease, consistent with the drop in support acidity.

The time online concentration profiles upon reuse of 1 wt% Ru/H-ZSM5(NH_3, A, 11.5) are shown in Fig. 3. The 1 wt% Ru/H-ZSM5(NH_3, A, 11.5) catalyst was assessed in two consecutive runs, then followed by a third run after a regeneration step involving coke burn-off at 723 K under a dilute hydrogen flow. While complete LA conversion was observed within 1 h reaction time for all three runs, the yield of PA decreased from 91.3 to 66.4 mol% upon two consecutive 10 h runs, with a concomitant drop in PA productivity from 1.042 to 0.547 $mol_{PA}\ g_{Ru}^{-1}\ h^{-1}$ (Table 3). From the time-profile (Fig. 3b), it can be seen that not the conversion to GVL, but rather the GVL-PA step was slowed down, again pointing to GVL ring-opening step to be most difficult. Upon regeneration, the spent catalyst recovered after two runs gave an increase in PA yield to 81.2 mol% in the third run, indicating that PA production activity of the catalyst could be almost completely restored by simple coke burn-off.

After regeneration, a bimodal particle size distribution was observed for Ru/H-ZSM5(NH_3, A, 11.5) with high angle annular dark field scanning TEM imaging (HAADF), showing small particles (<2 nm) as well as larger particles (ranging from 5 to 14 nm) located on the external surface of ZSM5 (Fig. S4). This bimodal distribution points at a significant fraction of ruthenium being originally located inside the zeolite pores.

While some sintering does take place, the fact that PA yields can be almost completely restored shows that the strong acidity of the ZSM5 must be mostly recovered upon regeneration. The TPD measurements show that the spent catalysts in three consecutive runs maintain the total acidity of the fresh one (Table 4), suggesting that Al leaching is very limited under the applied reaction conditions and that the coke that is deposited does not block the accessibility of the acid sites for ammonia. The overall strength of the acid sites is reduced upon the first and second run, however, as some of the strong acid sites are converted to weak acid sites and the remaining strong sites are on average less strong (Table 4, entry 1–3 and Fig. S3). The spent catalyst after the 3rd run shows a number of strong acid sites that is larger than that of the spent catalyst after the 2nd run, and almost the same as the spent catalyst after the 1st run (Table 4, entry 2, 3, 5). Compared to the spent catalyst of the first run, the shift of the HT peak maximum of the spent regenerated catalyst from 670 K to 651 K (Table 4, entry 2, 5) suggests, however, that a small amount of aluminum is irreversibly converted to extra-framework species during reaction and regeneration. Additionally, most of the coke (89%) could be removed in the regeneration step, fully recovering the porosity of the fresh Ru/H-ZSM5(NH_3, A, 11.5) (Table 4, entry 1, 4). Taken together, these results show that coke formation is the

Table 4
Physicochemical properties of fresh Ru/H-ZSM5(NH_3, A, 11.5) and spent catalyst after reaction at 473 K, 40 bar after 10 h in dioxane.

	Catalyst of 1 wt% Ru/H-ZSM5	BET (m^2/g)	Micropore surface area (m^2/g)	Micropore volume (cm^3/g)[a]	Mesopore volume (cm^3/g)[a]	Average Ru particle size (nm)[b]	Ru dispersion ZSM5[c]	Coke contents (wt%)[d]	LT Maximum (K)	Amount of weak acid sites ($mmol/g_{cat}$)	HT maximum (K)	Amount of strong acid sites ($mmol/g_{cat}$)	Total acid amount ($mmol/g_{cat}$)
1	Fresh (NH_3, A, 11.5)	324	251	0.12	0.07	1.7 ± 0.4	0.76		517	0.12	686	0.48	0.60
2	Spent after 1st run	137	107	0.05	0.03	3.8 ± 0.9	0.34	7.6	555	0.16	670	0.43	0.59
3	Spent after 2nd run	91	77	0.04	0.03	6.9 ± 2.1	0.19	9.9	536	0.24	667	0.35	0.59
4	Regenerated after 2nd run	333	246	0.12	0.08	5.8 ± 2.5	0.22	1.1					
5	Spent after 3rd run								576	0.17	651	0.42	0.59

[a] Data obtained by the t-plot method.
[b] Data obtained by TEM.
[c] Data estimated by TEM: D = 6*(vm/am)/d. Where vm is bulk metal atomic density of Ru (13.65×10^{-3} nm^3), am is the surface area occupied by an atom on a polycrystalline surface of Ru (6.35×10^{-2} nm^2), d is the cluster size of Ru metal.
[d] Data determined by TGA.

main reason for deactivation, as it weakens the acid strength and blocks the accessibility of ZSM5.

4. Conclusions

A highly active and selective bifunctional 1 wt% Ru/H-ZSM5 catalyst was developed for the direct, one-pot conversion of levulinic acid to pentanoic acid. Exploration of various synthesis parameters, including ruthenium precursor salt and cation form of the zeolite, resulted in a simple preparation method for catalysts with an improved dispersion of ruthenium, localized also in the pores of the zeolite, as well as an improved amount and strength of strong acid sites. The 1 wt% Ru/H-ZSM5 catalyst gives an excellent yield of 91.3% PA under relatively mild conditions and shows the highest productivity of 1.157 $mol_{PA}\ g_{Ru}^{-1}\ h^{-1}$ reported to date. Better control over the density of in particular strongly acidic sites was key to achieve this high productivity, as these sites are needed for the most difficult step in the tandem conversion of LA to PA. The new preparation method furthermore improves the proximity between the hydrogenation and ring-opening/dehydration functions of the catalyst, as a result of the deposition of small Ru clusters into the pores of ZSM5, which is beneficial for PA production. Deactivation of 1 wt% Ru/H-ZSM5(NH_3, A, 11.5) is primarily caused by carbon residue deposition on the strong acid sites.

Acknowledgments

The authors gratefully thank the Smart Mix Program of the Netherlands Ministry of Economic Affairs and the Netherlands Ministry of Education, Culture, and Science within the framework of the CatchBio Program for financial support. Cor van der Spek (TEM), Nazila Masoud (N_2 physisorption), Rafael de Lima Oliveira (N_2 physisorption), and Marjan Versluijs-Helder (TGA), all from Utrecht University, are acknowledged for the measurements.

Appendix A. Supplementary material

Supplementary data associated with this article can be found, in the online version, at http://dx.doi.org/10.1016/j.jcat.2014.09.014.

References

[1] J.J. Bozell, G.R. Petersen, Green Chem. 12 (2010) 539–554.
[2] J.J. Bozell, L. Moens, D.C. Elliott, Y. Wang, G.G. Neuenscwander, S.W. Fitzpatrick, R.J. Bilski, J.L. Jarnefeld, Resour. Conserv. Recy. 28 (2000) 227–239.
[3] D.W. Rackemann, W.O.S. Doherty, Biofuel. Bioprod. Bior. 5 (2011) 198–214.
[4] I.T. Horvath, H. Mehdi, V. Fabos, L. Boda, L.T. Mika, Green Chem. 10 (2008) 238–242.
[5] V. Pace, P. Hoyos, L. Castoldi, P. Domínguez de María, A.R. Alcántara, ChemSusChem 5 (2012) 1369–1379.
[6] J.-P. Lange, R. Price, P.M. Ayoub, J. Louis, L. Petrus, L. Clarke, H. Gosselink, Angew. Chem. Int. Ed. 49 (2010) 4479–4483.
[7] R. Palkovits, Angew. Chem. Int. Ed. 49 (2010) 4336–4338.
[8] J.C. Serrano-Ruiz, D. Wang, J.A. Dumesic, Green Chem. 12 (2010) 574–577.
[9] W. Luo, U. Deka, A.M. Beale, E.R.H. van Eck, P.C.A. Bruijnincx, B.M. Weckhuysen, J. Catal. 301 (2013) 175–186.
[10] T. Pan, J. Deng, Q. Xu, Y. Xu, Q.-X. Guo, Y. Fu, Green Chem. 15 (2013) 2967–2974.
[11] F. Lónyi, A. Kovács, J. Valyon, J. Phys. Chem. B 110 (2006) 1711–1721.
[12] L. Xin, Z. Zhang, J. Qi, D.J. Chadderdon, Y. Qiu, K.M. Warsko, W. Li, ChemSusChem 6 (2013) 674–686.
[13] J.C. Serrano-Ruiz, R.M. West, J.A. Dumesic, Annu. Rev. Chem. Biomol. Eng. 1 (2010) 79–100.
[14] J.J. Verdonck, P.A. Jacobs, M. Genet, G. Poncelet, J. Chem. Soc., Faraday Trans. 76 (1980) 403–416.
[15] C.V. Hidalgo, H. Itoh, T. Hattori, M. Niwa, Y. Murakami, J. Catal. 85 (1984) 362–369.
[16] F. Lónyi, J. Valyon, Micropor. Mesopor. Mater. 47 (2001) 293–301.
[17] S.M. Campbell, D.M. Bibby, J.M. Coddington, R.F. Howe, R.H. Meinhold, J. Catal. 161 (1996) 338–349.
[18] V.I. Pârvulescu, S. Coman, P. Palade, D. Macovei, C.M. Teodorescu, G. Filoti, R. Molina, G. Poncelet, F.E. Wagner, Appl. Surf. Sci. 141 (1999) 164–176.

[19] R.M. Dalla Betta, M. Boudart, in: J. Hightower (Ed.), Proceedings of the 5th International, Congress on Catalysis, Amsterdam, North-Holland, 1973, 1329.
[20] D.J. Elliott, J.H. Lunsford, J. Catal. 57 (1979) 11–26.
[21] L.A. Pedersen, J.H. Lunsford, J. Catal. 61 (1980) 39–47.
[22] S. You, I. Baek, Y. Kim, K.-E. Jeong, H.-J. Chae, T.-W. Kim, C.-U. Kim, S.-Y. Jeong, T. Kim, Y.-M. Chung, S.-H. Oh, E. Park, Korean J. Chem. Eng. 28 (2011) 744–750.
[23] P. Treesukol, K. Srisuk, J. Limtrakul, T.N. Truong, J. Phys. Chem. B 109 (2005) (1945) 11940–11945.
[24] C. Zhao, J.A. Lercher, Angew. Chem. Int. Ed. 51 (2012) 5935–5940.
[25] G.L. Woolery, G.H. Kuehl, H.C. Timken, A.W. Chester, J.C. Vartuli, Zeolites 19 (1997) 288–296.
[26] E.G. Derouane, J. Catal. 100 (1986) 541–544.
[27] E. Kikuchi, H. Nakano, K. Shimomura, Y. Morita, J. Jpn. Pet. Inst. 28 (1985) 210–213.
[28] M. Brändle, J. Sauer, J. Am. Chem. Soc. 120 (1998) 1556–1570.
[29] A. Vjunov, M.Y. Hu, J. Feng, D.M. Camaioni, D. Mei, J.Z. Hu, C. Zhao, J.A. Lercher, Angew. Chem. Int. Ed. 53 (2014) 479–482.